Journal of Solid Mechanics Vol. 12, No. 3 (2020) pp. 521-538
DOI: 10.22034/jsm.2019.573380.1320

The Effects of Initial In-Plane Loads on the Response of Composite-Sandwich Plates Subjected to Low Velocity Impact: Using a New Systematic Iterative Analytical Process

K. Malekzadeh Fard *, A.H. Azarnia

Department of Aerospace Engineering, Malek-e-Ashtar University of Technology, Tehran, Iran

Received 30 March 2020; accepted 25 May 2020

ABSTRACT

A new systematic iterative analytical procedure is presented to predict the dynamic response of composite sandwich plates subjected to low-velocity impact phenomenon with/without initial in-plane forces. In this method, the interaction between indenter and sandwich panel is modeled with considering the exponential equation similar to the Hertzian contact law and using the principle of minimum potential energy and the energy-balance model. In accordance with the mentioned procedure and considering initial in-plane forces, the unknown coefficients of the exponential equation are obtained analytically. Accordingly, the traditional Hertzian contact law is modified for use in the composite sandwich panel with the flexible core under biaxial pre-stresses. The maximum contact force using the two-degrees-of-freedom (2DOF) spring-mass model is calculated through an iterative systematic analytical process. Using the present method, in addition to reducing the runtime, the problem-solving process is carried out with appropriate convergence. The numerical results of the analysis are compared with the published experimental and theoretical results. The effects of some important geometrical and physical parameters on contact force history are examined in details.

Keywords: Low-velocity impact; Composite sandwich plate; New analytical contact law; Initial in-plane force.

1 INTRODUCTION

THE main reasons using composite and sandwich structures in various industries (e.g. aerospace, maritime and road transportation, civil and mechanical structures) are specific strength and bending stiffness, lightweight, thermal insulation, etc. One of the serious issues limiting the applications of sandwich structures is the sensitivity of these materials to impact with external objects. Damage due to impact behavior on the sandwich panel can lead to the reduction in compressive strength structure. For this reason, the problem of impact is significantly effective in

*Corresponding author. Tel.: +91 9378171222.
E-mail address: Kmalekzadeh@mut.ac.ir (K. Malekzadeh Fard).

designing and manufacturing sandwich panels. In sandwich structures containing a lightweight core, indentation is strongly influenced by the core. This is because deformation predominately occurs by crushing the soft core for sandwich structures consisting of high-stiffness face sheets and a flexible core [1]. Extensive research carried out on the low energy impact response on composite and sandwich structures. Liou [2] achieved the contact law for carbon/epoxy composite impacted by rigid sphere through indentation experimental test. In the corresponding paper, three models were considered for contact law, including $F = K\alpha^{1.5}, F = K\alpha^{1.2}, F = K\alpha^{n}$. In the third equation, the values of k and n were determined based on applying least squares method on the obtained results. The results indicated that as the thickness of the plate increases, the value of the exponent parameter of Hertzian law decreases. Yang and Sun [3] studied indentation phenomena through static indentation tests on graphite/epoxy multilayer plates. The obtained results are similar to the experimental Hertz's relationship. It was concluded that value 1.5 is suitable for value n. Lee [4] carried out indentation tests to establish the contact law for a $12.7mm$ spherical diameter steel indenter on a sandwich structure. Based on tests, the value of the contact coefficient for loading phase was 0.8. Olsson [5] developed an analytical model for contact indentation of sandwich panel. It was deduced that the exponential parameter in the Hertzian contact law for the sandwich panel is equal to 1. the contact law in the sandwich structures is fundamentally different from that in metallic structures. With increasing transverse in the sandwich panel, the core becomes crushed. Therefore, in these types of structures, core crushing is significant. Turk and HooFatt [6] analytically investigated indentation of an indenter into a rectangular sandwich-composite plate, considering the core crushing. Using appropriate shape function for the top face sheet, the elastic strain energy of the sandwich plate, dissipated plastic work resulted from crushing the core and the external work due to impact force were calculated. Sburlati [7] studied the force–indentation response associated with a rigid particle influencing a sandwich structure. It was deduced that a Hertzian contact pressure distribution is not suitable for low-density systems. Choi et al. [8] proposed a new approach using linearized contact law to analyze of impact behavior on the composite structure and compared it to modified Hertzian contact law. It was shown that the linearized contact law can be valuable for solving the impact analysis problems. Kiratisaevee and Cantwell [9] carried out indentation and dynamic tests on aluminum foam sandwich panels and fiber-metal laminate sandwich panels. They found that the parameter n for aluminum foam-based sandwich structures varies between 0.9 and 1.2 and between 0.7 and 0.9 for fiber-metal laminate sandwich structures. The average value of C for dynamic loading was significantly higher than that for the quasi-static data. A few studies on the low velocity impact on the composite and the sandwich structure have been reported under in-plane load. The effects of the initial in-plane stresses and the transverse flexibility of the core of the sandwich panel, using improved higher-order sandwich plate theory have been investigated by Malekzadeh et al. [10]. It was shown that as tensile in-plane initial stresses increase, indentation force increase but total first contact time decrease. Choi [11] introduced a finite element equation based on the modified displacement field to solve dynamic response of the composite structure considering initially loaded in-plane stresses. Due to the obtained results and compared to compressive in-plane load, it can be seen that the initial tensile in-plane induced the fast response. Hossini et al. [12] derived an improved contact law for the deformation response of sandwich panel indented by a rigid flat-ended cylindrical impactor. The load- indentation response is derived by using minimization of total potential energy. In this paper, the effects of In-plane forces on impact response were investigated. It is observed that the positive initial in-plane forces decrease the indentation but increase the slope of the indentation force versus top face-sheet deflection curve. Static indentation of the composite-sandwich plate is analytically investigated by Khalili et al. [13]. The effect of in-plane displacement component as well as the in-plane forces acting on the edge of the sandwich panel are incorporated in the mentioned analysis. In this study, as the in-plane biaxial tension is applied simultaneous to the structure, result more changes in the indentation curve than as only one of the forces is applied. Shariyat et al. [14] investigated the low-velocity impact of sandwich structure with viscoelastic cores under biaxial pre-loading. The result indicated that with increasing initial velocity of the indenter, due to viscoelastic nature of the core the contact force decrease and an opposite trend was observed in the absorbed energy.

In this paper, a new modified contact law is introduced to investigate the low-velocity impact response of the sandwich plates. In this method, assuming the exponential equation similar to the Hertzian contact law, using the principle of minimum potential energy and the energy-balance model between the indenter and the sandwich plate, the unknown coefficients of the exponential equation are analytically obtained. Considering that initial in-plane forces are important in determining the response of the structure, thus the effects of these forces on the impact behavior of the sandwich panel are investigated. In addition, the effects of some important geometrical and physical parameters on the contact force history were discussed in detail.

2 ANALYTICAL FORMULATION

The composite sandwich flat panel of dimension $a \times a$ studied in this paper, is composed of the symmetric face-sheets and a core with thickness h_c as shown in Fig.1. The panel is subjected low-velocity impact a blunt end cylindrical indenter with radius *R* and length *L* at normal obliquity. In this work, the friction between panel and impactor is assumed to be negligible. Also, the effects of secondary contact loading are assumed to be negligible. In this article, the simultaneous application of the biaxial tensile (or compressive) and the shear load on impact response of sandwich panel is survived. *t* can be assumed that the in-plane normal and shear loads act along the panel edges statically. In order to investigate the local indentation of the panel, the analysis considers indentation of a panel resting on a rigid foundation [15]. It is assumed that face sheet indentation becomes less than about half of the plate thickness [6]. When the core is crushed with a constant force resistance per unit area, *q*, the foundation is termed as rigid-plastic. As the core layer is flexible and weak along in-plane direction, it cannot accept in-plane loads along its edge. Here, the in-plane loads are carried only by the face-sheets. Fig. 2 shown the assumed distribution of the initial in-plane force [13]. According to the classic laminate plate theory, the elastic strain energy due to the bending of an orthotropic laminated face sheet is:

$$U = 1/2 \iint D_{11}\left(\frac{\partial^2 \omega}{\partial x^2}\right)^2 + D_{22}\left(\frac{\partial^2 \omega}{\partial y^2}\right)^2 + 2D_{12}\left(\frac{\partial^2 \omega}{\partial x^2}\right)\left(\frac{\partial^2 \omega}{\partial y^2}\right) + 4D_{12}\left(\frac{\partial^2 \omega}{\partial x^2}\right)\left(\frac{\partial^2 \omega}{\partial y\,\partial x}\right) + 4D_{26}\left(\frac{\partial^2 \omega}{\partial y^2}\right)\left(\frac{\partial^2 \omega}{\partial x\,\partial y}\right) + 4D_{66}\left(\frac{\partial^2 \omega}{\partial x\,\partial y}\right) \Big\} d_A \tag{1}$$

In which D_{ij} is the laminated bending stiffness, $d_A = d_x d_y$ and *A* is the surface area of the deformed face sheet. As shown in Fig.3, the profile of the local indentation of the upper face sheet can be approximated by the following function [16]:

$$\alpha = \begin{cases} \delta & for\ 0 \le x^2 + y^2 \le R^2 \\ \delta\left[(1-(\frac{x-R}{\xi-R})^2\right]^2\left[(1-(\frac{y-R}{\xi-R})^2\right]^2 & \\ for \quad R^2 < x^2 + y^2 < \xi^2 \ x > 0, y > 0 & \end{cases} \tag{2}$$

where δ is the deflection under the indenter, and ξ is the lateral extent of the deformation zone [6]. It is assumed that the mentioned profile satisfies the boundary condition.

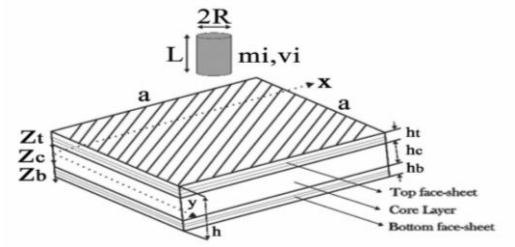

Fig.1
Geometry of the composite sandwich panel.

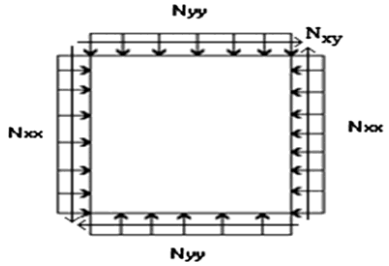

Fig.2
Distribution of the in-plane forces.

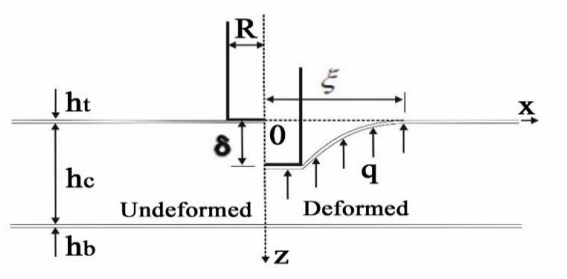

Fig.3
Schematic profile of the deforming and the undeforming zone.

Substituting Eq. (2) into Eq. (1) gives:

$$U = \frac{D_1 \delta^2}{(R-\xi)^2} \tag{3}$$

where

$$D_1 = \frac{65536}{11025}[\frac{7}{4}D_{11} + \frac{7}{4}D_{22} + D_{12} + 2D_{66}] \tag{4}$$

The minimum total potential energy principle is used to analyze the relation. The total potential energy can be written in the form of:

$$\Pi = U + D - W \tag{5}$$

In which D is the plastic work dissipated in crushing the core and W is the work done by the indentation force. The plastic work due to compressive deformation of the core is defined by summing the work done under the indenter (D_1^*) and outside the indenter in the deforming zone (D_2). (See Fig. 3).

$$D \approx D_1^* + D_2 = \pi q R^2 \delta + 4\int_R^{\xi}\int_R^{\xi} q\,\delta d_x d_y \tag{6}$$

where q is the crushing strength of the core. By inserting the shape function Eq. (2) into Eq. (6) and integrating the result we will have:

$$D = \pi q R^2 \delta + \frac{256}{225} q\,\delta (R-\xi)^2 \tag{7}$$

The vectors of the in-plane forces along the edge of the top and bottom face-sheet and the vector of the in-plane resultant forces along the edges of the panel are respectively as follows:

$$\left[N^t\right] = \begin{bmatrix} N_{xx}^t \\ N_{yy}^t \\ N_{xy}^t \end{bmatrix}, \quad \left[N^b\right] = \begin{bmatrix} N_{xx}^b \\ N_{yy}^b \\ N_{xy}^b \end{bmatrix} \quad \left[\bar{N}\right] = \begin{bmatrix} \bar{N}_{xx} \\ \bar{N}_{yy} \\ \bar{N}_{xy} \end{bmatrix} \xrightarrow{where} [\bar{N}] = [N^b] + [N^t] \tag{8}$$

where N_{xx}^i, N_{yy}^i and N_{xy}^i $(i = t, b)$ are the initial in-plane forces acting on the edge of the sandwich panel. By taking into account the effect of initial in-plane normal and shear loads and assuming an even distribution for the indentation load on the contact area, the external work done is given by:

$$W = \int_0^{2\pi}\int_0^R \frac{F\delta}{\pi R^2} r d_r d_\theta - 2\int_R^\xi\int_R^\xi (N_{xx}^t (\frac{\partial\omega}{\partial x})^2 + N_{yy}^t (\frac{\partial\omega}{\partial y})^2 + N_{xy}^t (\frac{\partial\omega}{\partial x})(\frac{\partial\omega}{\partial y}))d_x d_y$$
$$\rightarrow W = F\delta - \frac{32768\delta^2}{33075}(N_{xx}^t + N_{yy}^t) - \delta^2 N_{xy}^t \quad (9)$$

where F is indentation force. Since, the core is assumed to be rigid-plastic, therefore the in-plane forces applied to the bottom face-sheet have no contribution in the total potential energy. The indentation behavior of the sandwich structure can be approximated using non-linear exponential equation, which states:

$$F = K\alpha^n \quad (10)$$

where α and K are the indentation index and the contact stiffness, respectively. In the present study, K and n are constants which were determined analytically using a new systematic iterative process. The energy absorbed in the contact area can be expressed as:

$$E_c = \int_0^{\alpha_{\max}} K\alpha^n d_\alpha = \frac{K\alpha_{\max}^{n+1}}{n+1} = \frac{(\frac{F_{\max}}{\alpha^n})\alpha_{\max}^{n+1}}{n+1} = \frac{F_{\max}\alpha_{\max}}{n+1} \quad (11)$$

In which $F_{\max}$ is the maximum indentation force. It is assumed that an average force during impact path are defined. The force is applied in the quasi-static form. As a result, the work done due to the mentioned force is defined as follow [16]:

$$\bar{W} = F^*\alpha_{\max} \quad (12)$$

By equalizing Eq. (12) with the work done by the indentation force, Eq. (11), we will have:

$$F^* = \frac{F_{\max}}{n+1} \quad (13)$$

where F^* is the average force. Calculating the total potential energy of the sandwich plate during the indentation process and minimizing it with respect to the central deflection i.e., δ yields the contact force:

$$\frac{2D_1\delta}{(R-\xi)^2} + \pi qR^2 + \frac{256}{225}q(R-\xi)^2 + \frac{65536\delta}{33075}(N_{xx}^t + N_{yy}^t) + 2\delta N_{xy}^t = \frac{F_{\max}}{n+1} \quad (14)$$

To simplify the calculation, the following terms are assumed:

$$\pi qR^2 + \frac{256}{225}q(R-\xi)^2 = N$$
$$\frac{2D_1\delta}{(R-\xi)^2} + \frac{65536\delta}{33075}(N_{xx}^t + N_{yy}^t) + 2\delta N_{xy}^t = M \quad (15)$$

As a result:

$$F_{\max} = M(n+1)\delta + N(n+1) \rightarrow F_{\max} = M(n+1)(\frac{F_{\max}}{K})^{\frac{1}{n}} + N(n+1) \quad (16)$$

Considering the above equation based on K, we will have:

$$K^{\frac{-1}{n}} = \left(\frac{F_{\max}^{\frac{n-1}{n}}}{M(n+1)}\right) - \frac{N}{M} F_{\max}^{\frac{-1}{n}} \tag{17}$$

2.1 Energy balance model

When the composite-sandwich panel is simply supported around the edge, two types of deformation occur: the Local deformation of the top face sheet into the core, δ , which was analyzed in the previous section and the global plate bending and shear deformation, Δ. Here we develop an energy balance model to achieve a new relationship based on parameters $F_{\max}$ and k . Based on the assumption of quasi-static behavior, the initial energy of the impactor is equal to the sum of the energies due to localized indentation in the contact area together with global deformation [15]. The global deformation usually includes bending, shear and membrane deformations in the panel. The energy balance model neglecting the membrane effect can be written as:

$$\frac{1}{2} m_i v_i^2 = E_c + U \tag{18}$$

where m_i and v_i are the mass and initial velocity of the impactor, respectively, U is the bending and shear strain energy and E_c is the indentation energy in the contact area. The indentation energy can be expressed as:

$$E_c = \int_0^{\alpha_{\max}} F d\alpha = \frac{K \alpha_{\max}^{n+1}}{n+1} = \frac{K^{\frac{-1}{n}} F_{\max}^{\frac{n+1}{n}}}{n+1} \tag{19}$$

The principle of minimum energy is again utilized to derive and approximate solution for the global deformation. The function related to transverse deformation is, W, and the rotation with respect to the x-and y-axis, $\bar{\alpha}$ and $\bar{\beta}$ can be defined as follows.

$$\begin{aligned} w &= \Delta f(x) f(y) \quad \frac{-a}{2} \le x \le \frac{a}{2}, \ \frac{-a}{2} \le y \le \frac{a}{2} \\ \bar{\alpha}(x,y) &= \alpha_0 g(x) h(y) \quad \frac{-a}{2} \le x \le \frac{a}{2}, \ \frac{-a}{2} \le y \le \frac{a}{2} \\ \bar{\beta}(x,y) &= \beta_0 h(x) g(y) \quad \frac{-a}{2} \le x \le \frac{a}{2}, \ \frac{-a}{2} \le y \le \frac{a}{2} \end{aligned} \tag{20}$$

In which Δ , α_0 and β_0 are the amplitudes of shape functions for transverse deflection and rotations. Functions $f(x)$, $f(y)$, $g(x)$, $h(x)$, and $g(y)$, are selected to satisfy the displacement and force boundary condition at the edges. The strain energy for the symmetric sandwich panel by neglecting the in-plane deformation with respect to the transverse deformation is as:

$$\begin{aligned} U = 4 \int_0^{a/2} \int_0^{a/2} \Bigg\{ & \frac{D_{11}}{2} \left(\frac{\partial \bar{\alpha}}{\partial x}\right)^2 + D_{12} \left(\frac{\partial \bar{\alpha}}{\partial x}\right)\left(\frac{\partial \bar{\beta}}{\partial x}\right) + \frac{D_{22}}{2} \left(\frac{\partial \bar{\beta}}{\partial x}\right)^2 + D_{66} \left[\frac{1}{2} \left(\frac{\partial \bar{\alpha}}{\partial y}\right)^2 + \left(\frac{\partial \bar{\alpha}}{\partial y}\right)\left(\frac{\partial \bar{\beta}}{\partial x}\right) + \frac{1}{2} \left(\frac{\partial \bar{\beta}}{\partial x}\right)^2 \right] + \\ & D_{16} \left[\left(\frac{\partial \bar{\alpha}}{\partial x}\right)\left(\frac{\partial \bar{\alpha}}{\partial y}\right) + \left(\frac{\partial \bar{\alpha}}{\partial x}\right)\left(\frac{\partial \bar{\beta}}{\partial x}\right) \right] + D_{26} \left[\left(\frac{\partial \bar{\alpha}}{\partial y}\right)\left(\frac{\partial \bar{\beta}}{\partial y}\right) + \left(\frac{\partial \bar{\beta}}{\partial x}\right)\left(\frac{\partial \bar{\beta}}{\partial y}\right) \right] + \\ & A_{55} \left[\frac{\bar{\alpha}}{2} + \frac{\bar{\alpha}\,\partial \omega}{\partial x} + \frac{1}{2} \left(\frac{\partial \omega}{\partial x}\right)^2 \right] + A_{44} \left[\frac{\bar{\beta}}{2} + \frac{\bar{\beta}\,\partial \omega}{\partial y} + \frac{1}{2} \left(\frac{\partial \omega}{\partial y}\right)^2 \right] \Bigg\} d_x d_y \end{aligned} \tag{21}$$

where D_{ij}^s is the bending stiffness matrix and A_{44}^s and A_{55}^s are the transverse shear stiffness of the panel. The superscript "*s*" denotes the sandwich panel. If *h*<<*H*, the transverse shear stiffness is given as $A_{44}^s = A_{55}^s = G_{13}H$, where G_{13} is the shear modulus of the core. Substituting the derivatives of the expression in Eq. (20) into Eq. (21) gives the strain energy in terms of Δ , α_0 and β_0 as follows:

$$U = A_1\Delta^2 + A_2\Delta\beta_0 + A_3\beta_0^2 + A_4\Delta\alpha_0 + A_5\alpha_0^2 + A_6\alpha_0\beta_0 \tag{22}$$

where

$$\begin{aligned} A_1 &= \frac{2240}{1575}[A_{44} + A_{55}], \quad A_2 = \frac{1344}{1575}[A_{44}a] \\ A_3 &= \frac{1}{1575}[204a^2A_{44} + 2016D_{22} + 2040D_{66}] - D_{26} \\ A_4 &= \frac{1344}{1575}[A_{55}a], \quad A_5 = \frac{1}{1575}[204a^2A_{55} + 2016D_{11} + 2040D_{66}] - D_{16} \\ A_6 &= \frac{4032}{1575}[D_{12} + D_{66} + D_{16}] - D_{26} \end{aligned} \tag{23}$$

The external work is defined as:

$$V = 4\int_0^{a/2}\int_0^{a/2} \frac{P\Delta}{a^2} d_x d_y - 2\int_0^{a/2}\int_0^{a/2} (N_{xx}^t (\frac{\partial\omega}{\partial x})^2 + N_{yy}^t (\frac{\partial\omega}{\partial y})^2 + N_{xy}^t (\frac{\partial\omega}{\partial x})(\frac{\partial\omega}{\partial y}))d_x d_y \tag{24}$$

Therefore, the total potential energy is:

$$\begin{aligned} \Pi &= U - V = A_1\Delta^2 + A_2\Delta\beta_0 + A_3\beta_0^2 + A_4\Delta\alpha_0 + A_5\alpha_0^2 + A_6\alpha_0\beta_0 \\ &-P\Delta + (\frac{18}{64}N_{xy}^t - \frac{36}{5}N_{yy}^t - \frac{82}{60}N_{xx}^t)\Delta^2 \end{aligned} \tag{25}$$

To simplify the calculation, the following term is assumed:

$$(\frac{18}{64}N_{xy}^t - \frac{36}{5}N_{yy}^t - \frac{82}{60}N_{xx}^t) = L_0 \tag{26}$$

Minimizing Π with respect to Δ , α_0 and β_0, the equilibrium of the system is obtained as:

$$\begin{aligned} &\frac{\partial\pi}{\partial\alpha_0} = 0 \rightarrow A_4\Delta + 2A_5\alpha_0 + A_6\beta_0 = 0 \\ &\frac{\partial\pi}{\partial\beta_0} = 0 \rightarrow A_2\Delta + A_6\alpha_0 + 2A_3\beta_0 = 0 \\ &\frac{\partial\pi}{\partial\Delta} = 0 \rightarrow 2A_1\Delta + A_4\alpha_0 + A_2\beta_0 - P + 2\Delta L_0 = 0 \end{aligned} \tag{27}$$

By solving the above system of equations and defining parameters such as $A_7, A_8, A_9, A_{10}, A_{11}, A_{12}$ and A_{13} , the parameter values for Δ , α_0 and β_0 are achieved as follows:

$$A_7 = A_2 - \frac{2A_3A_4}{A_6}, \quad A_8 = A_6 - \frac{2A_5A_2}{A_6}, \quad A_9 = (2A_1 + L_0) - \frac{A_2A_4}{A_6}, \quad A_{10} = A_4 - \frac{2A_2A_5}{A_6}$$
$$A_{11} = \frac{1}{A_{10} - \frac{2A_9A_8}{A_7}}, \quad A_{12} = -\frac{A_{11}A_8}{A_7}, \quad A_{13} = -\left[\frac{A_4A_{12}}{A_6} + \frac{2A_5A_{11}}{A_6}\right] \tag{28}$$

Then:

$$\alpha_0 = A_{11}F^*, \ \beta_0 = A_{13}F^*, \ \Delta = A_{12}F^* \tag{29}$$

Substituting Eq. (30) in to Eq. (23) gives:

$$U = \left\{A_1A_{12}^2 + A_2A_{12}A_{13} + A_3A_{13}^2 + A_5A_{11}^2 + A_4A_{12}A_{11} + A_6A_{11}A_{13}\right\} * (F^*)^2 \tag{30}$$

Substituting Eq. (13) in to Eq. (30) gives:

$$U = A_{14}\frac{F_{\max}}{(n+1)^2} \tag{31}$$

In which:

$$A_{14} = \left\{A_1A_{12}^2 + A_2A_{12}A_{13} + A_3A_{13}^2 + A_5A_{11}^2 + A_4A_{12}A_{11} + A_6A_{11}A_{13}\right\} \tag{32}$$

Now, by inserting Eqs. (19) and (31) into Eq. (18), the equation of energy-balance is rewritten as follows:

$$\frac{1}{2}m_i v_i^2 = A_{14}\frac{F_{\max}}{(n+1)^2} + \frac{K^{\frac{-1}{n}}F_{\max}^{\frac{n+1}{n}}}{n+1} \tag{33}$$

Considering Eq. (33) based on K, we will have:

$$K^{\left(-\frac{1}{n}\right)} = \left[\frac{1}{2}(n+1)m_i v_i^2 F_{\max}^{\frac{n+1}{-n}} - \left(\frac{A_{14}}{n+1}\right)F_{\max}^{\left(\frac{n-1}{n}\right)}\right] \tag{34}$$

By equating the two independent values obtained of parameter K (Eq. (18) and Eq. (35)), we have:

$$F_{\max} = \frac{\frac{N}{M}(n+1) + \left(\frac{N^2}{M^2}(n+1)^2 + 4T(n+1)^2\left(\frac{1}{M} + A_{14}\right)\right)^{0.5}}{2\left(\frac{1}{M} + A_{14}\right)} \tag{35}$$

where $T = \frac{1}{2}m_i v_i^2$. It is observed in Eq. (32), that maximum force is a function of the unknown parameter (n). In addition, contact stiffness can be obtained in terms of exponent parameter, n, using Eq. (31). Here, the main issue is to obtain the maximum impact force.

2.2 Calculating the maximum contact force

In this study, the two-degrees-of-freedom (TDOF) spring-mass model is proposed and employed to predict maximum contact force. According to Fig. 4, the set of equations of motion of the TDOF system is as follows:

$$\left\{\begin{array}{c} m_i \ddot{x}_1 + k^*\left(X_1 - X_2\right) = 0 \\ m_s \ddot{x}_2 - k^*\left(X_1\right) + \left(k_g + k^*\right) X_2 = 0 \end{array}\right\} \tag{36}$$

where m_i and m_s are the effective mass of the impactor and the sandwich panel, respectively. K^* and K_g are the linearized contact coefficient in Choi`s linearized contact law and the dynamic global stiffness of the sandwich panel. Furthermore, $X_1$ and $X_2$ are the displacements of the impactor and the structure, respectively. In the above equation, using Choi`s linearized model [8], instead of the nonlinear Hertzian contact law, the contact force can be obtained as:

$$F\left(t\right) = K^*\alpha = K^*\left(x_2 - x_1\right), \qquad K^* = K^{\frac{1}{n}} F_{\max}^{\frac{n-1}{n}} \tag{37}$$

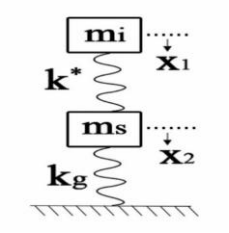

Fig.4
The two-degree-of-freedom model.

Using Eq. (27) K_g is obtained as:

$$K_g = \frac{F^*}{\Delta} = \left[\begin{array}{l} \left(4\left\{A_1 + \frac{64}{45}\left[N_{xx}^t + N_{yy}^t\right] + N_{xy}^t\right\} A_5 - A_4^2\right)\left(4A_3A_5 - A_6^2\right) \\ + \left(2A_2A_3 - A_4A_6\right)\left(A_4A_6 - 2A_2A_5\right) \end{array}\right] \tag{38}$$

The initial conditions of Eq. (36) are as follows:

$$t = 0 \longrightarrow x_1 = x_2 = 0, \qquad \mathrm{x}_1^0 = v_{i,} \qquad \mathrm{x}_2^0 = 0 \tag{39}$$

Considering Eq. (36), the displacement of the impactor and sandwich panel can be written as:

$$x_1 = C_1 \sin \omega t, \qquad x_2 = C_2 \sin \omega t, \tag{40}$$

Substituting Eq. (40) into Eq. (38), we will have:

$$\begin{pmatrix} k^* - m_i\omega^2 & -k^* \\ k^* & -(k^* + k_g - m_s) \end{pmatrix}\begin{pmatrix} c_1 \\ c_2 \end{pmatrix} = \begin{pmatrix} 0 \\ 0 \end{pmatrix} \tag{41}$$

Using Eq. (41), the natural frequency can be expressed as follows:

$$\omega_{1,2}^2 = \frac{\left[m_i\left(k^* + k_g\right) - k^* m_s\right] \pm \left[\left(m_i\left(k^* + k_g\right) - k^* m_s\right) - 4m_i k^* m_s k_g\right]^{0.5}}{2m_i m_s} \tag{42}$$

The mode shape can be obtained as:

$$\left(\frac{A_1}{A_2}\right)_1 = \frac{k^*}{k^* - m_i\omega_1^2} = \Phi_0^1 = \begin{pmatrix} \Phi_0 \\ 1 \end{pmatrix}^1, \left(\frac{A_1}{A_2}\right)_2 = \frac{k^*}{k^* - m_i\omega_2^2} = \Phi_0^2 = \begin{pmatrix} \Phi_0 \\ 1 \end{pmatrix}^2 \tag{43}$$

Φ_0^1 and Φ_0^2 are the first and second mode shapes, respectively. The motion`s equation of the spring-mass system can be written as follows:

$$\begin{pmatrix} x_1 \\ x_2 \end{pmatrix} = C_1 \begin{pmatrix} \Phi_0 \\ 1 \end{pmatrix}^1 \sin\left(\omega_1 t + \psi_1\right) + C_2 \begin{pmatrix} \Phi_0 \\ 1 \end{pmatrix}^2 \sin\left(\omega_2 t + \psi_2\right) \tag{44}$$

Because there is no damper in the system, $\psi_1 = \psi_1 = 0$, by applying the boundary condition (Eq. (39)).

$$C_1 = \frac{v_0}{\omega_1\left(\Phi_0^1 - \Phi_0^2\right)}, \qquad C_1 = \frac{v_0}{\omega_1\left(\Phi_0^2 - \Phi_0^1\right)} \tag{45}$$

Finally, using (Eq. (45) and Eq. (44)), the contact force history can be achieved as follows:

$$F\left(t\right) = k^*\left(x_2 - x_1\right) = k^*\left(C_1\Phi_0^1 \sin\left(\omega_1 t\right) + C_2\Phi_0^2 \sin\left(\omega_2 t\right)\right) \tag{46}$$

To obtain the maximum contact force, $F_{\max}$, we take the first derivative of Eq.(46) as follows:

$$\frac{dF\left(t\right)}{dt} = \omega_1 C_1\left(\Phi_0^1 - 1\right)\cos\left(\omega_1 t^*\right) + C_2\omega_2\left(\Phi_0^2 - 1\right)\cos\left(\omega_2 t^*\right) = 0 \tag{47}$$

Afterwards, by substituting the maximum obtained contact time *(t^*)* in Eq. (46), the corresponding maximum contact force can be obtained. Also, substituting maximum contact force into Eq. (37), the linearized contact stiffness can be achieved. The process for obtaining the modified contact law is shown in Appendix A. In the modified contact law, the maximum impact force between the impactor and the impacted surface of the target structure during the impact is first estimated, after that using Eqs. (35) and (37), parameters *K* and *n* are obtained. Again, using Eq. (46), maximum contact time is calculated. Finally, maximum contact force is achieved using Eq. (46) and previous value is compared. Then, process continues until convergence. In Eq. (36), the effective mass of the target structure can be approximated by assuming that the velocity profile is similar to the deformation profile for the sandwich panel [6].

The kinetic energy (KE) is as follow:

$$KE = 2\int_0^{\frac{a}{2}} \int_0^{\frac{a}{2}} \rho_s\left(h_t + h_b + h_c\right)\overset{0}{\Delta}{}^2 \left[1 - \left(\frac{2x}{a}\right)^2\right]\left[1 - \left(\frac{2y}{b}\right)^2\right] d_x d_y \tag{48}$$

where ρ_s is the mass density of the sandwich panel. After integration of Eq. (48), *KE* is:

$$KE = \frac{32}{225}\rho_s\left(h_t + h_b + h_c\right)a^2\,\overset{0}{\Delta}{}^2 \tag{49}$$

The *KE* using the effective sandwich mass m_s is also given as:

$$KE = \frac{1}{2} m_s\,\overset{0}{\Delta}{}^2 \tag{50}$$

Therefore, the effective sandwich panel mass is:

$$m_s = \frac{64}{225}\rho_s\left(h_t + h_b + h_c\right)a \tag{51}$$

3 VALIDATION AND RESULTS

3.1 Model validation

In this section, the low-velocity impact response of rectangular sandwich panel made of AS4/3501-6 carbon/epoxy face sheets and Nomex honeycomb core with/without initial in-plane forces will be investigated. The panel is subjected to the low-velocity impact of a hemispherical-nose cylindrical impactor made of casehardened steel with the radius of R and length of L. Dimensions of the structure as well as the material and geometrical properties of the face sheet, core and indenter are stated in Tables 1-2. It is assumed that the stacking sequence of laminate used in the present analysis in the top and bottom face sheets is considered as $[0,90]_{8s}$. In order to consider the effect of strain rates, the dynamic stiffness of the face sheets is assumed to be equal to its static value, while the dynamic crushing strength of the core of the sandwich structure is 10% higher than the static value [6]. Based on the governing Eq. (46), the impact force history curve for the mentioned composite sandwich panel is plotted in Fig. 5 and compared with the experimental results obtained from Shokrieh et al. [17] as well as the analytical results reported by Hoo Fatt and Park [6] and Malekzadeh et al. [10]. It is obvious that the peak load predicted by the present analytical result about 0.85% less than the result obtained by the experimental test, while this discrepancy is about 5% and 8.2% for the analytical results reported by Hoo Fatt andPark [6] and Malekzadehet al.[10], respectively.

Table 1
Material and geometrical properties of composite sandwich plates and the impactor.

Face-sheet	Core
$a \times a = 178 \times 178 mm^2$	$\rho_c = 64 kg/m^3$ (density)
$h_k = 0.0635$ (ply thickness)	$d = 3.2 mm$ (cell diameter)
$\rho_f = 1632 kg/m^3$ (mass density)	$h_c = 12.7 mm$ (core thickness)
Ply stiffness	$q = 3.83 Mpa$ (crushing resistance)
$E_{11} = 144.8 Gpa$ ($longitudinal\ stiffness$)	$D = 25.4 mm$ (diameter)
$E_{22} = 9.7 Gpa$ ($transverse\ stiffness$)	$L = 660 mm$ (length)
$G_{12} = 7.1 Gpa$ ($in-plane\ shear$ modulus)	$M_0 = 3.48 kg$ (mass)
$\vartheta_{11} = 0.3$ ($poission's\ ratio$)	$V_0 = 1.42\ m/s$ (initial velocity)

Table 2
Mechanical properties of HRH/8-4.0 Nomex honeycomb.

properties
$E_{11} = E_{22} = 80.4 Mpa$ (in-plane stiffness)
$E_{33} = 1.005 Gpa$ (transverse stiffness)
$G_{12} = 32.2 Mpa$ (in-plane shear modulus)
$G_{23} = 75.8 Mpa$ (out-plane shear modulus)
$G_{13} = 120.6 Mpa$ (out-plane shear modulus)
$\vartheta_{12} = 0.25$ (Poisson's ratio)
$\vartheta_{13} = 0.2$ (Poisson's ratio)
$\vartheta_{23} = 0.2$ (Poisson's ratio)

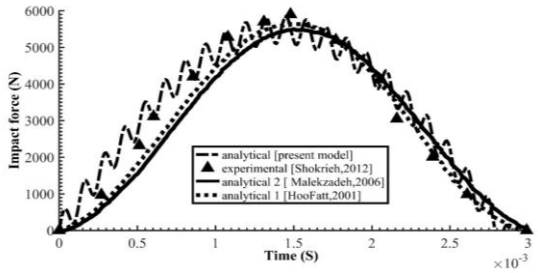

Fig.5
Impact force vs. time for carbon/epoxy composite sandwich plate subjected to hemispherical-nose cylinder.

Based on the present model, effect of the in-plane initial tensile stresses on the force vs. time curve is illustrated in Fig.6. Accordingly, if the zero in-plane force values are considered as the reference, i.e. $N_{xx} = N_{xy} = N_{yy} = 0$, then by applying these forces to the sandwich panel subjected to low-velocity impact, the maximum contact force will be increased, while simultaneously the contact duration will be reduced. Furthermore, the results shown in Fig.6 are in good agreement with those obtained in [10].

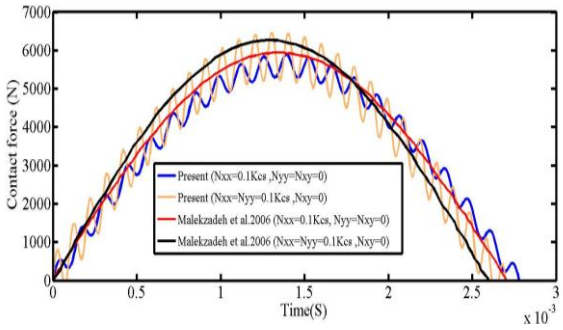

Fig.6
The effect of the in-plane initial tensile stresses on the force vs. time curve.

As seen in Fig.7, the value of the tensile preload from 0 to $600\frac{m}{s}$ is increased. By increasing initial in-plane force values, the maximum contact force is increased. In addition, according to Fig.7 the effect of increase initial in-plane force values on the contact stiffness parameter, *k*, and the power parameter, *n*, of the modified exponential equation are shown in Table 3. It is observed that with increasing the initial in-plane forces, the contact stiffness parameter, *k*, is increased, while the power parameter, *n*, is reduced. Obviously, it can be concluded from Fig.7 that the increase of the contact force is due to the increasing of the contact stiffness parameter *k*.

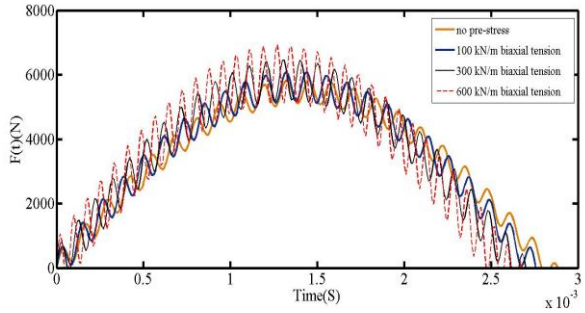

Fig.7
The variation of the contact force history of the sandwich panel in various initial in-plane forces.

Table 3
The effect of the in-plane initial tensile stresses on the contact stiffness and the power parameter.

In-plane initial stresses $\frac{kN}{m}$	Maximum contact force $F_{\max}(kN)$	The contact stiffness $K(\frac{kN}{m^n})$	The power parameter n
No pre-stress	5.85	5.36e6	0.8
$N_x = N_y = 100\ (\frac{kN}{m})$	6.08	6.29e6	0.79
$N_x = N_y = 300\ (\frac{kN}{m})$	6.45	8.23e6	0.78
$N_x = N_y = 600\ (\frac{kN}{m})$	6.82	1.12e7	0.76

3.2 Effect of mass and velocity of impactor in a constant impact energy level with/without in-plane forces

Effect of different masses and velocities of the impactor in a constant impact energy level is shown in Fig.8. It is assumed that the mass and velocity are equal to 3.48 *kg* and 1.42 *m/s*, 6.96 *kg* and 1 *m/s*, 10.44 *kg* and 0.82 *m/s*,

respectively. All of mentioned cases are in a constant impact energy level of 3.51 *J*. At a constant impact energy level, regardless of the in-plane forces, the maximum contact force of curve is reduced by decreasing the velocity of the impactor (from Curve 1 to Curve 3 and from Curve 3 to Curve 5), while the contact duration is increased from 2.67 *ms* to the minimum 4.67 *ms*. By applying the tensile preload $N_x = N_y = 300\ (\frac{kN}{m})$, the maximum contact force in curve 1 compared to the previous one about 10 percent is reduced, while this reduction is about 8 percent for curve 3. It is also observed that, the effective parameter in reducing the contact force based on $F = k\alpha^n$ equation is indentation, α .

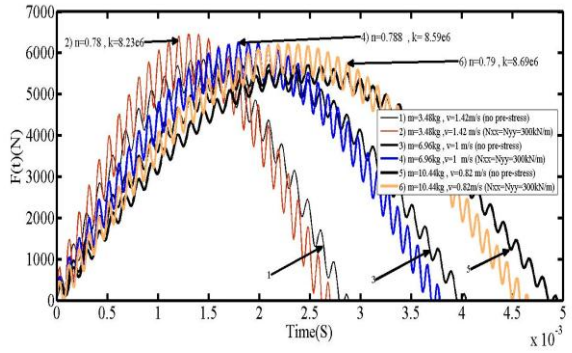

Fig.8
Effect of various mass and velocity values of the impactor in a constant energy level with/without initial in-plane forces.

3.3 Effect of core thickness-to-sandwich panel thickness ratio with/without in-plane forces on low-velocity impact response

In order to find the effect of the core thickness-to-sandwich panel thickness ratio, $\frac{h_c}{h}$, different values of parameter $\frac{h_c}{h}$ were selected so that, in each case, the force vs. time curves (Fig.9) and indentation vs. time curve (Fig.10) were illustrated with/without considering the initial in-plane forces. The obtained results demonstrated that with an increase in the core thickness, the flexibility of the structure is increased, thus, the contact duration is reduced, while the maximum contact time is increased.

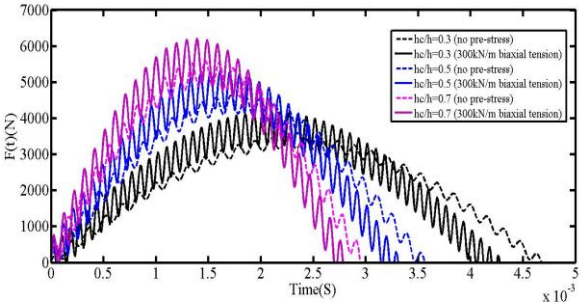

Fig.9
The effect of the core thickness-to-sandwich panel thickness ratio, $\frac{h_c}{h}$, with/without initial in-plane forces on maximum contact force.

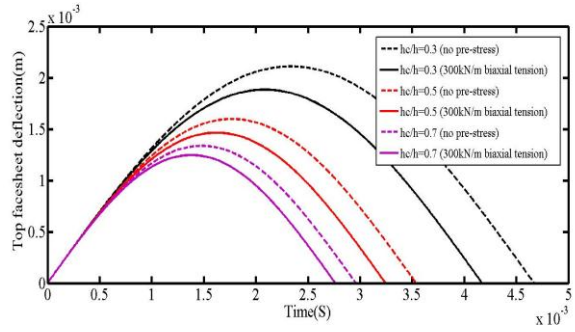

Fig.10
The effect of the core thickness-to-sandwich panel thickness ratio, $\frac{h_c}{h}$, with/without initial in-plane forces on top facesheet deflection.

3.4 Effect of thickness of face sheet on low-velocity impact response in sandwich panel with initial tensile preload

In Table 4, effects of four different types of the stacking sequence of laminate forces on the maximum contact force and maximum indentation with $300\frac{kN}{m}$ biaxial tension forces are investigated. Characteristics of the impactor and target structure are in accordance with Tables 1-2. The thickness of all layers in the face sheets of the panels is assumed identical and equal to 0.0635 *mm*. The mass of the impactor is 3.48 *kg* and the tip of the impactor has a diameter of 25.4 *mm*. When the thickness of laminate increases, the contact force increases as well. According to Table 5, the value of k increases but the value of n decreases as the thickness (flexural rigidity) of the skin increases. According to Table 4, with increasing the number of plies and ply thickness, the indentation on the top face sheet is reduced. Therefore, thicker laminates have the least indentation. As a result, it is clear that contact stiffness 'k' and parameter 'n' are dependent on laminate thickness.

Table 4
Effect of laminate thickness on modified contact laws with initial in-plane forces.

Lamination	k	n	$F_{\max}(N)$	$\alpha_{\max}(m)$
$A:[0_3,90_3,0_3]$	5.695×10^6	0.8266	5453.0	2.2277×10^{-4}
$B:[0_4,90_4,0_4]$	5.917×10^6	0.8223	5719.3	2.1565×10^{-4}
$C:[0_5,90_5,0_5]$	6.073×10^6	0.8154	5973.1	2.0511×10^{-4}
$D:[0_6,90_6,0_6]$	6.1859×10^6	0.8117	6031.7	1.9523×10^{-4}

3.5 Indentation variations for sandwich panel due to the low-velocity impact in the presence of the initial in-plane forces

Fig. 11 shows the effect of velocity of the impactor on the indentation of the sandwich structure considering the initial in-plane forces. In Fig.11, if the initial in-plane force of zero is considered as the reference, the indentation in sandwich panel will be reduced by applying the force. Due to the similarity of the velocity variations for all of the applied forces, only the large diameter depicted in the elliptical shapes is reduced. Therefore, by applying larger values of the in-plane forces, it can be concluded that the elliptical shapes will be inclined toward the circular shapes. It is interesting to note that, when the impactor's velocity approaches zero, the maximum indentation will be obtained.

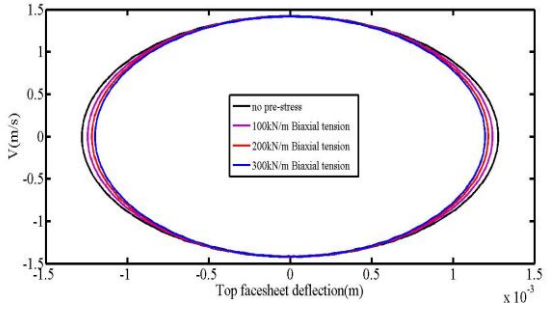

Fig.11
The variation of the indentation of the sandwich panel in various velocities with inital in-plane forces.

3.6 Effect of in-plane-tensile forces on response of sandwich panel subjected to low-velocity impact

Force-time curve of the sandwich plate for different values of in-plane tensile forces is illustrated in Fig.12. If the in-plane forces of zero are considered as the reference, it can be seen from the figure that when the in-plane forces such as N_{xx} , N_{yy} and N_{xy} are applied to the sandwich panel simultaneously, larger changes will be observed in the force vs. time curve until N_{xx} or N_{yy} are applied to the panel alone. Similarly, when the forces N_{xx} and N_{yy} are applied to the panel at the same time, the maximum contact force will be more changes in comparison with the case in which N_{xx} or N_{yy} are applied to the panel alone. Obviously, it can be concluded from Fig.12 that as the in-plane

forces such as N_{xx} , N_{yy} and N_{xy} are applied to the sandwich panel simultaneously, maximum contact force about 10 percent is reduced in comparison with the case in which N_{xx} or N_{yy} are applied to the structure alone.

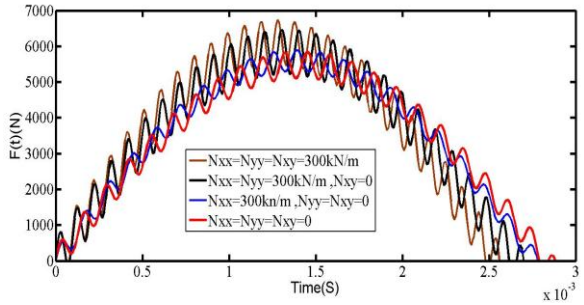

Fig.12
Impact force history for the different values of the initial in-plane forces.

3.7 Effect of $\frac{a}{h}$ *parameter on dynamic response of sandwich panel with/without the initial in-plane forces*

Fig.13 shows the effect of the length-to-thickness ratio $\frac{a}{h}$ of the square-sandwich panel on dynamic response of sandwich panel with/without considering the initial in-plane forces. As observed in this figure, with increasing the dimensionless parameter $\frac{a}{h}$ and simultaneous use of the in-plane forces, the power parameter (n) is reduced. In the case of $\frac{a}{h}=16$, the difference of the results obtained from the cases with/without considering the in-plane forces for power parameter n will be insignificant and it seems that with a further increase in parameter $\frac{a}{h}$, effect of the in-plane forces on parameter (n) can be neglected. However, Fig.14 has a different status in terms of parameter k, since it seems that there is a difference even in the value of greater length-to-thickness ratio. As a result, in the presence of the initial in-plane forces, the effect of parameter k on the parameter $\frac{a}{h}$ will be significant.

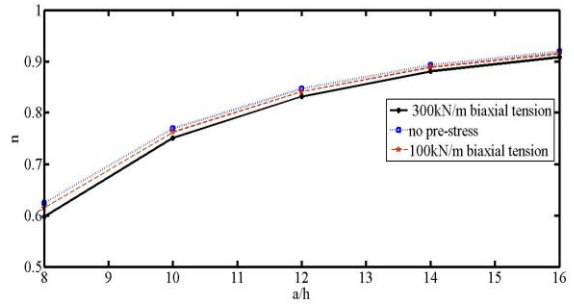

Fig.13
Effect of $\frac{a}{h}$ parameter on the power parameter, n, of the modified exponential equation with/without the initial in-plane forces.

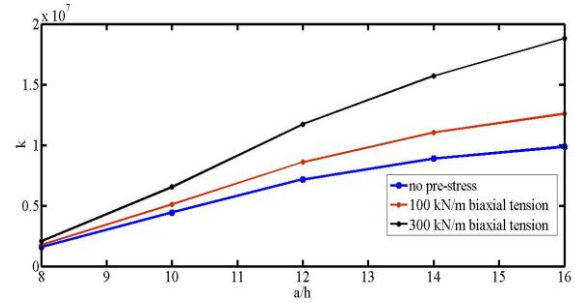

Fig.14
Effect of $\frac{a}{h}$ parameter on the contact stiffness parameter, k , of the modified exponential equation with/without the initial in-plane forces.

3.8 Effect of initial tensile forces on the contact force indentation relationship

Fig. 15 shows the effect of considering the initial in-plane forces on the force-indentation curve based on power-law contact force indentation relationship ($F = K\alpha^n$). As it can be observed, the power parameter (n) is reduced by increasing the in-plane forces from curve 1 to curve 4, while the contact stiffness parameter k and the maximum contact force are increased. It is interesting to note that, according to Fig.15 by increasing the initial in-plane forces, the curves approach the y-axis.

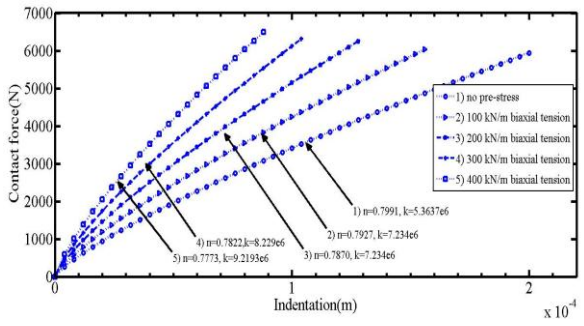

Fig.15
Effect of initial tensile forces on the contact force indentation relationship.

4 CONCLUSIONS

For most sandwich panels, the local deformation of the core dominates the global deflection due to a low-modulus core. Consequently, the traditional Hertzian contact law should be modified to cater for sandwich panels. In this paper, a new systematic iterative analytical process for the low-velocity impact analysis of composite sandwich plates with/without initial in-plane forces was presented.

In this method, using the principle of minimum potential energy and the energy-balance model between the indenter and the sandwich plate, the unknown coefficients of the exponential equation were obtained analytically assuming exponential equations such as the Hertzian contact law. The maximum contact force using the 2DOF spring-mass model was found through an iterative systematic analytical process. By presenting the exponential equation in which coefficients are calculated analytically, the process of solving is performed in less time. In order to study the effect initial in-plane forces upon the panel, it is assumed that the in-plane normal and shear loads act along the top face sheets edges statically. The validity of the present formulation is verified with existing analytical models and experimental results. Due to the flexibility of the core, the impact force history curves are different from the ones predicted by the Hertzian contact law. In addition, due to the crushing of the core soft, with the increase in the indentation of sandwich structures, the exponent parameter of the traditional Hertzian law decreases. For the considered case, the results showed that the impactor's velocity is a more effective parameter in the maximum contact force at constant energy levels in comparison with the mass of the impactor. When the impact energy level increases, the maximum impact force and the contact duration increase, although the values of contact coefficient, k and n of the modified contact law decrease. In addition, it can be concluded that as the in-plane forces are applied to the sandwich panel simultaneously, maximum contact force in comparison with the case in which initial in-plane forces are applied to the structure alone, is reduced. It is also observed that the variation of contact force-indentation relation approaches linearity when face sheet thickness decreases.

The results indicated that some geometrical parameters, e.g. the length-to-thickness ratio $\left(\frac{a}{h}\right)$, the core thickness-to-panel thickness ratio $\frac{h_c}{h}$, kinetic energy, and initial velocity of the impactor, are important factors with the greatest influence on contact coefficients and impact process.

The results showed that, in the presence of the initial in-plane forces, the effect of parameter k on the parameter $\frac{a}{h}$ would be significant while with increase in parameter $\frac{a}{h}$, effect of the in-plane forces on parameter (n) can be neglected.

APPENDIX A

The process to obtain the new analytical method.

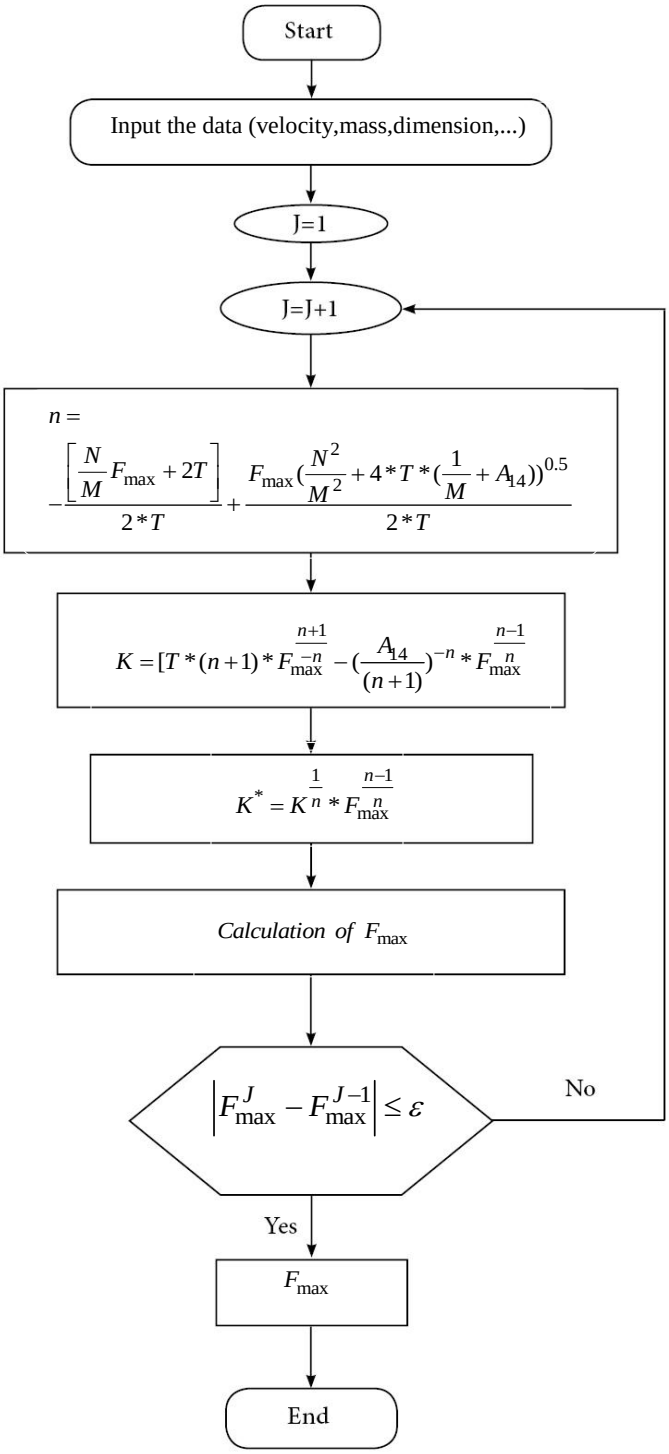

REFERENCES

[1] Koller M.G., 1986, Elastic impact of spheres on sandwich plates, *Zeitschrift für Angewandte Mathematik und Physik (ZAMP)* **37**(2): 256-269.

[2] Lee L.J.,Huang K.Y., Fann Y.J., 1993,Dynamic responses of composite sandwich plate impacted by a rigid ball, *Journal of Composite Materials* **27**(13): 1238-1256.

[3] Yang S.H., Sun C.T., 1982,Indentation law for composite laminates, *ASTM STP* **787**: 425-449.

[4] Olsson R., McManus H.L., 1996, Improved theory for contact indentation of sandwich panels, *AIAA* **34**(6): 1238-1244.

[5] Liou W.J., 1997,Contact laws of carbon/Epoxy laminated Composite plates, *Journal of Reinforced Plastics and Composites* **16**: 155-166.

[6] Hoo Fatt M.S., Park K.S., 2001, Dynamic models for low-velocity impact damage of composite sandwich panels-part A: Deformation, *Composite Structure* **52**: 335-351.

[7] Sburlati R., 2002,The effect of a slow impact on sandwich plates, *Journal of Composite Materials* **36**(9): 1079-1092.

[8] Choi I.H.,Lim C.H., 2004, Low velocity impact analysis of composite laminates using linearized contact law, *Composite Structures* **66**: 125-132.

[9] Kiratisaevee H., Cantwell W.J., 2005, Low-velocity impact response of high-performance aluminum foam sandwich structures, *Journal of Reinforced Plastics and Composites* **24**(10): 1057-1072.

[10] Malekzadeh K.,Khalili M.R.,Mittal R.K., 2006, Response of in-plane linearly prestressed composite sandwich panels with transversely flexible core to low-velocity impact, *Journal of Sandwich and Materials* **8**: 157-181.

[11] Choi I.H., 2008, Low-velocity impact analysis of composite laminates under initial in-plane load, *Journal of Composite Structures* **86**: 251-257.

[12] Hossini M.,Khalili M.R.,Malekzadeh K., 2011,Indentation analysis of in-plane prestress composite sandwich plates: An improved contact law, *Key Engineering Materials* **471-472**: 1159-1164.

[13] Khalili M.R.,Hosseini M.,Malekzadeh K., Forooghgy S.H., 2013, Static indentation response of an in-plane pre-stressed composite sandwich plate subjected to a rigid blunted indenter, *European Journal of Mechanics A/Solids* **38**: 59-69.

[14] Shariyat M.,Hosseini S.H., 2014, Eccentric impact analysis of pre-stressed composite sandwich plates with viscoelastic cores: A novel global–local theory and a refined contact law, *Composite Structures* **117**: 333-345.

[15] Zhou D.W.,Stronge W.J., 2006, Low velocity impact denting of HSSA lightweight sandwich panel, *International Journal of Mechanical Sciences* **48**: 1031-1045.

[16] Azarnia A.H.,Malekzadeh K., 2018, Analytical modeling to predict dynamic response of Fiber-Metal Laminated Panel subjected to low velocity impact, *Journal of Science and Technology of Composite* **5**(3): 331-342.

[17] Shokrieh M.M.,Fakhar M.N., 2012, Experimental, analytical, and numerical studies of composite sandwich panels under low-velocity impact loadings, *Mechanics of Composite Materials* **47**(6): 643-658.